Pergamon

Neuroscience Vol. 91, No. 4, pp. 1445–1460, 1999

PII: S0306-4522(98)00665-4
0306-4522/99 $20.00+0.00

BURST FIRING IN IDENTIFIED RAT GENICULATE INTERNEURONS

J. J. ZHU,* D. J. UHLRICH* and W. W. LYTTON†‡

*Department of Anatomy, Neuroscience Training Program, University of Wisconsin, Madison, WI 53706, U.S.A.

†Department of Neurology, Neuroscience Training Program, University of Wisconsin, and Wm. S. Middleton VA Hospital, 1300 University Avenue, Madison, WI 53706, U.S.A.

Abstract—We used whole-cell patch recording to study 102 local interneurons in the rat dorsal lateral geniculate nucleus *in vitro*. Input impedance with this technique (607.0 ± 222.4 MΩ) was far larger than that measured with sharp electrode techniques, suggesting that interneurons may be more electrotonically compact than previously believed. Consistent and robust burst firing was observed in all interneurons when a slight depolarizing boost was given from a potential at, or slightly hyperpolarized from, resting membrane potential. These bursts had some similarities to the low-threshold spike described previously in other thalamic neuron types. The bursting responses were blocked by Ni^+, suggesting that the low-threshold calcium current I_T, responsible for the low-threshold spike, was also involved in interneuron burst firing. Compared to the low-threshold spike of thalamocortical cells, however, the interneuron bursts were of relatively long duration and low intraburst frequency. The requirement for a depolarizing boost to elicit the burst is consistent with previous reports of a depolarizing shift of the I_T activation curve of interneurons relative to thalamocortical cells, a finding we confirmed using voltage-clamp. Voltage-clamp study also revealed an additional long-lasting current that could be tentatively identified as the calcium activated non-selective cation current, I_{CAN}, based on reversal potential and on pharmacological characteristics. Computer simulation of the interneuron burst demonstrated that its particular morphology is likely due to the interaction of I_T and I_{CAN}. In the slice, bursts could also be elicited by stimulation of the optic tract, suggesting that they may occur in response to natural stimulation. Synaptically triggered bursts were only partially blocked by Ni^+, but could then be completely blocked by further addition of (±)-2-amino-5-phosphonopentanoic acid. The existence of robust bursts in this cell type suggests an additional role for interneurons in sculpting sensory responses by feedforward inhibition of thalamocortical cells.

The low-threshold spike is a mechanism whereby activity in a neuron is dependent on a prior lack of activity in that same neuron. Understanding of the low-threshold spike in the other major neuron types of the thalamus has brought many new insights into how thalamic oscillations might be involved in sleep and epilepsy. Our description of this phenomenon in the interneurons of the thalamus suggests that these network oscillations might be even more complicated than previously believed. © 1999 IBRO. Published by Elsevier Science Ltd.

Key words: thalamus, inhibition, vision, epilepsy.

The thalamic dorsal lateral geniculate nucleus (LGN) is the primary structure that relays visual information from the retina to the cortex in mammals.[66,68] In addition, the thalamus is involved in normal and abnormal synchronized neural activity.[36,71,72,76,81–83] These sensory and oscillatory functions are mediated by three basic types of neurons:[41] thalamocortical (TC) cells, local intrageniculate interneurons and cells in the adjacent thalamic reticular nucleus (RE). TC cells are excitatory neurons, and they alone have axons that project to the cortex. In contrast, interneurons and RE cells are GABAergic, and their axons project locally within the thalamus to exert considerable inhibitory influence on TC cells.[79] The inhibition provided by these two cell types is important for sculpting ascending visual signals,[56,70] and for promoting and synchronizing the thalamic oscillations.[76]

In contrast to TC and RE cells, local interneurons are much less studied, and the limited data from *in vivo* and *in vitro* studies have sometimes been contradictory. Interneurons studied *in vitro* have generally shown regular spiking in response to current clamp, burst behavior being observed only inconsistently.[5,43,52,59,84] By contrast, reports from *in vivo* studies have suggested that putative interneurons can produce bursts as well as regular firing

‡To whom correspondence should be addressed at 1300 University Avenue.

Abbreviations: DL-APV, (±)-2-amino-5-phosphonopentanoic acid; EGTA, ethyleneglycolbis(aminoethyl ether)tetra-acetate; EPSP, excitatory postsynaptic potential; HEPES, *N*-2-hydroxyethylpiperazine-*N*′-2-ethanesulfonic acid; IPSP, inhibitory postsynaptic potential; LGN, lateral geniculate nucleus; LTS, low-threshold spike; NMDA, *N*-methyl-D-aspartate; $NMDG^+$, *N*-methyl-D-glucamine; RE, thalamic reticular nucleus; RMP, resting membrane potential; TC, thalamocortical.

in response to stimulation of the optic tract.[1,11,15,21,63,77] Furthermore, putative interneurons tended to fire bursts of action potentials during sleep states and produced regular firing during waking.[63] Of course, these *in vivo* studies have been largely extracellular and have not provided anatomical definition of the cells observed.

Earlier *in vitro* results suggested that thalamic interneurons had little or no I_T, the low-threshold calcium current. However, Pape *et al.*[58] recently used the whole-cell technique to demonstrate that dissociated LGN interneurons have a prominent I_T and can generate a low-threshold spike (LTS). The LTS did not, however, lead to a burst of action potentials in their dissociated interneurons. In the present study, we have performed whole-cell recordings of interneurons in slices, varying the standard LTS current-clamp protocol in order to take account of the altered voltage-dependent characteristics of I_T in interneurons.[58]

EXPERIMENTAL PROCEDURES

Slice preparation

Sprague–Dawley rats (Harlan, Indianapolis, IN; four to 10 weeks old; 100–300 g) were deeply anesthetized using halothane. A minimum number of animals were used to obtain the necessary results and the animals were not allowed to suffer in any way. After decapitation, the brain was quickly removed into cold (6–8°C) physiological solution containing (in mM): NaCl 126, KCl 2.5, NaH_2PO_4 1.25, $NaHCO_3$ 26, $MgSO_4$ 1, dextrose 20, $CaCl_2$ 2 (pH 7.35). The solution was continuously bubbled with 95% O_2/5% CO_2. Slices containing the LGN, each 500 μm thick, were cut from the tissue blocks with a microslicer. Slices were kept in an oxygenated physiological solution for at least 2 h before recording. During the recording, slices were submerged in a Plexiglas chamber and stabilized using a fine nylon net attached to a platinum ring.[19] The chamber was perfused with warmed, oxygenated physiological solution, and the half-time for the bath solution exchange was about 7 s. The temperature of the bath solution in the chamber was kept at 34.0 ± 0.5°C. Antagonists were applied with the bath solution.

Physiology

The methods for tight-seal patch recordings follow Hamill *et al.*,[26] with modifications for brain slices.[7,19,90] Patch electrodes were made from borosilicate tubing (1.2 μm o.d., 0.9 μm i.d.) using a horizontal puller (Sutter Instruments). Electrode resistances were 7–9 MΩ. The standard intracellular solution contained (in mM): $C_6H_{11}O_7K$ 120, HEPES 10, EGTA 5, $MgCl_2$ 2, ATP 4, GTP 0.1, $CaCl_2$ 0.5, KCl 10 and 0.25% biocytin (pH 7.25). To obtain whole-cell recordings, electrodes, pulsing with 0.1-nA current steps of 200 ms duration, were advanced into the slice. When a significant increase in electrode resistance was evident, gentle suction was applied to attain a seal resistance of 1 GΩ or greater. The patch of membrane was broken by applying more negative pressure to obtain a whole-cell configuration.

We used an Axoclamp-2A amplifier (Axon Instruments) to perform both current-clamp and voltage-clamp recordings. When recording in current-clamp mode, the bridge balance was continuously monitored and adjusted. Single-electrode continuous voltage-clamp studies were performed on the cells with access resistance <30 MΩ, and the series resistance was compensated by 75–85%. Electrodes of this caliber were required to consistently obtain interneuron recordings. During the voltage clamp, 4 μM tetrodotoxin, 500 μM 4-aminopyridine and 10 mM tetraethylammonium were also included in the bath solution. A P/5 protocol was used to subtract capacitance and leak currents. The optic tract was stimulated by a concentric bipolar electrode with single voltage pulses (200 μs, up to 9 V). A 10-mV liquid junction potential was subtracted from all membrane potentials.

Histology

After each recording, the slice was fixed by immersion in 4% paraformaldehyde in 0.1 M phosphate buffer and resectioned at 60 μm on a freezing microtome. Sections were processed histologically with the avidin–biotin–peroxidase method to reveal the cell morphology.[32] Cells were subsequently drawn with the aid of a camera lucida system.

Computer modeling

Computer modeling was performed on a Sun workstation using NEURON.[29] Our model interneuron had 15 cylindrical compartments, representing a soma, two equivalent proximal dendrites and 12 equivalent distal dendrites. The diameters (D) and lengths (L) of these cylinders, estimated from stained geniculate interneurons and adjusted to fit the membrane time constant obtained by a small current injection, are: $D_{soma} = 10$ μm and $L_{soma} = 16$ μm; $D_{proximal\ dendrite} = 3.25$ μm and $L_{proximal\ dendrite} = 240$ μm; $D_{distal\ dendrite} = 1.75$ μm and $L_{distal\ dendrite} = 180$ μm; $C_m = 1$ μF/cm^2; $R_i = 100$ Ωcm.

The parallel conductance model, as well as activation and inactivation variables, were parameterized using the standard Hodgkin–Huxley formulation. Calcium channels used the Goldman–Hodgkin–Katz formulation instead of a reversal potential. Intrinsic channels were simulated at a temperature of 36°C and inserted in the soma of the model cell only.

Inclusion of dendritic channels was assessed for selected simulations and did not alter the results significantly. This was not surprising given the compactness of the model cell. The intrinsic conductances included a leak conductance ($\bar{g}_{leak} = 0.008$ mS/cm^2, $E_{leak} = -72.5$ mV), the Traub modification of the Hodgkin–Huxley I_{Na} and I_{Kdr} (Borg–Graham parameterization[47]), as well as the following channels. I_H (a hyperpolarization-activated cation current) parameters were obtained from our voltage-clamp data:[89] $\bar{g}_h = 0.13$ mS/cm^2; $E_h = -44$ mV; $h_\infty = 1/(1+\exp[(V + 79.0)/7.4])$; $\tau_h = \exp[(V + 293.3)/29.67]/(1 + \exp[(V + 76.7)/7.82])$; h exponent = 1.

I_T (low-threshold calcium channel) values were obtained from previous voltage-clamp data.[58] Kinetics were corrected for temperature using $m_{Q10} = 3$ and $h_{Q10} = 1.5$ (23–36°C). $\bar{p}_T = 0.1$ cm/s (maximal permeability); $m_\infty = 1/(1+\exp[-(V+57)/4.8])$; $h_\infty = 1/(1+\exp[-(V+78)/4.6])$; $\tau_m = 2 + 1/(\exp[(V+42)/10] + \exp[(-V-100)/15])$; $\tau_h = 24 + 1/(\exp[(V+56)/3.2] + \exp[(-V-384)/51])$; m exponent = 2; h exponent = 1. I_L (high-threshold calcium current) was adapted from a previous study[42] with kinetics adapted to 36°C using $Q_{10} = 3$.

Calcium decay times were assumed to be similar to that measured by calcium imaging techniques in apical dendrites and spines of cortical or hippocampal pyramidal cells.[28,48,64,73,88] Due to preliminary data suggesting that I_{CAN} and I_{AHP} may have different sensitivities to calcium ions coming through the low-threshold and high-threshold calcium channels (see Results), two separate calcium pools were simulated with I_{CAN} receiving approximately 80% Ca^{2+} influence from I_T current and I_{AHP} receiving approximately 80% from I_L current. The two calcium pumps were identical, with two different time constants for high and low

Ca^{2+} concentrations:

$$[Ca^{2+}]_i' = -(75 \cdot ica/(2 \cdot F \cdot 0.1)) + (Ca_{inf1} - cai)/\tau_1 + (Ca_{inf2} - cai)/\tau_2.$$

I_{CAN} (calcium-activated cation current) was adapted from a previous study,[17] and modified to fit our voltage-clamp data: $E_{can} = 10$ mV, $\alpha = \alpha_0[Ca^{2+}]_i^n$/ms; $\alpha_0 = 1.4 \times 10^5/\mu M^8$; $\beta = 0.003$/ms; $n = 8$. I_{AHP} (calcium-activated potassium current) used the same parameterization, but with $\alpha_0 = 0.031/\mu M^2$, $\beta = 0.02$/ms and $n = 2$.

The time step for the simulations was typically set at 0.025 ms. Sometimes, a shorter time step (e.g., 0.01 or 0.005 ms) was used to repeat the same simulations. The results were nearly identical.

RESULTS

Neuronal identification

We recorded from 102 interneurons in the rat LGN using whole-cell patch recording technique. Of these, 40 were assessed for the burst firing reported in this study. Thalamic interneurons were identified physiologically and morphologically. Physiological identification was based on previously described criteria,[52,59,84] with some modification resulting from our use of the whole-cell technique. All cells were successfully labeled with biocytin, so that their identity could be confirmed morphologically.[22,23,57,84]

The morphology of an interneuron is compared to that of a cortically-projecting TC cell in Fig. 1. Interneurons generally had a bipolar appearance, with two dendrites arising from a relatively small soma. The interneuron dendrites were long, beaded and had intricate branching patterns. It was not always possible to distinguish the interneuron axon, being little different in light microscopic appearance from the many thin dendrites. In cases where the putative axon could be identified, the axonal and dendritic arbors tended to be spatially offset from each other, with the axon arbor occupying a relatively smaller area. By contrast, TC cells generally had a multipolar appearance, with five to eight relatively unelaborated dendrites radiating out from the soma (Fig. 1B).[22,23,57,84] In this figure, a stout axon, presumably destined for cortex, was transected at the edge of the slice.

In addition to morphological differences, local interneurons could be distinguished unambiguously from TC cells by their physiological properties (Fig. 1, insets). In the whole-cell preparation, interneurons showed a larger input resistance (607.0 ± 222.4 MΩ, S.D.) and longer time constant (94.0 ± 26.2 ms) in response to hyperpolarizing current. These values were both about five times higher than those seen in geniculate TC cells (118.7 ± 45.7 MΩ and 22.5 ± 7.1 ms; see Zhu and Uhlrich[90]) and four to five times higher than reported previously in interneurons. Resting membrane potential (RMP) in the interneurons was -67.7 ± 5.1 mV, compared to -71.4 ± 3.1 mV for TC cells.[90] Figure 1 also illustrates a key difference between the two cell types. TC cells always showed burst firing on release from hyperpolarization.[39,40] Using a similar protocol, interneurons usually did not.[54,90]

Burst responses of lateral geniculate nucleus interneurons

Although the standard hyperpolarization protocol used to obtain a burst in TC cells did not elicit a burst in interneurons, we could invariably obtain burst firing by using an alternative protocol, applying a small amount of depolarizing current following the hyperpolarization (Fig. 2). This requirement for a depolarizing boost helps explain why previous studies did not document a consistent burst response. The requirement for the boost is consistent with the voltage-clamp results of Pape *et al.*,[58] confirmed below. These results showed a shift in the activation curve of I_T in the depolarized direction. As we shall show that I_T is involved in the interneuron burst, this activation shift implies that a burst was, in most cases, only elicited at a depolarized state, rather than at the resting potential, in contrast to the LTS of TC cells. In many cells, the preceding hyperpolarization was not required and a burst could be elicited directly from RMP with depolarization (Fig. 2B, C).

Figure 3 illustrates representative bursts near threshold for a number of cells. Each trace is the first burst response in a progressive series of depolarizing pulses, with either no preceding hyperpolarization or only slight (<5 mV) hyperpolarization. Fast sodium action potentials rode on a slower, transient depolarizing spike, similar in appearance to the LTS of TC and RE cells.[3,4,13,39,53] For the majority of interneurons, the initial burst showed two to 16 action potentials. In cases where only a single action potential was elicited at low current (Fig. 3A–D), larger depolarizing pulses produced robust bursts of spikes.

Burst duration was typically 40–380 ms and terminated long before the end of the depolarizing current pulse. In five interneurons, however, the burst responses continued up to 700 ms after the termination of the depolarizing current step (e.g., Fig. 4B). In contrast to the fast intraburst firing of TC cells (Fig. 4E; generally ≥400 Hz), the average frequency within an interneuron burst ranged from 30 to 170 Hz (Fig. 4D). Although the probability of evoking a burst did not depend on a preceding hyperpolarization, the intensity of the burst, as measured by initial spike frequency, was greater if elicited from a more hyperpolarized potential (Fig. 4C). Burst duration was not consistently affected by the depth of the preceding hyperpolarization (Fig. 4A, B).

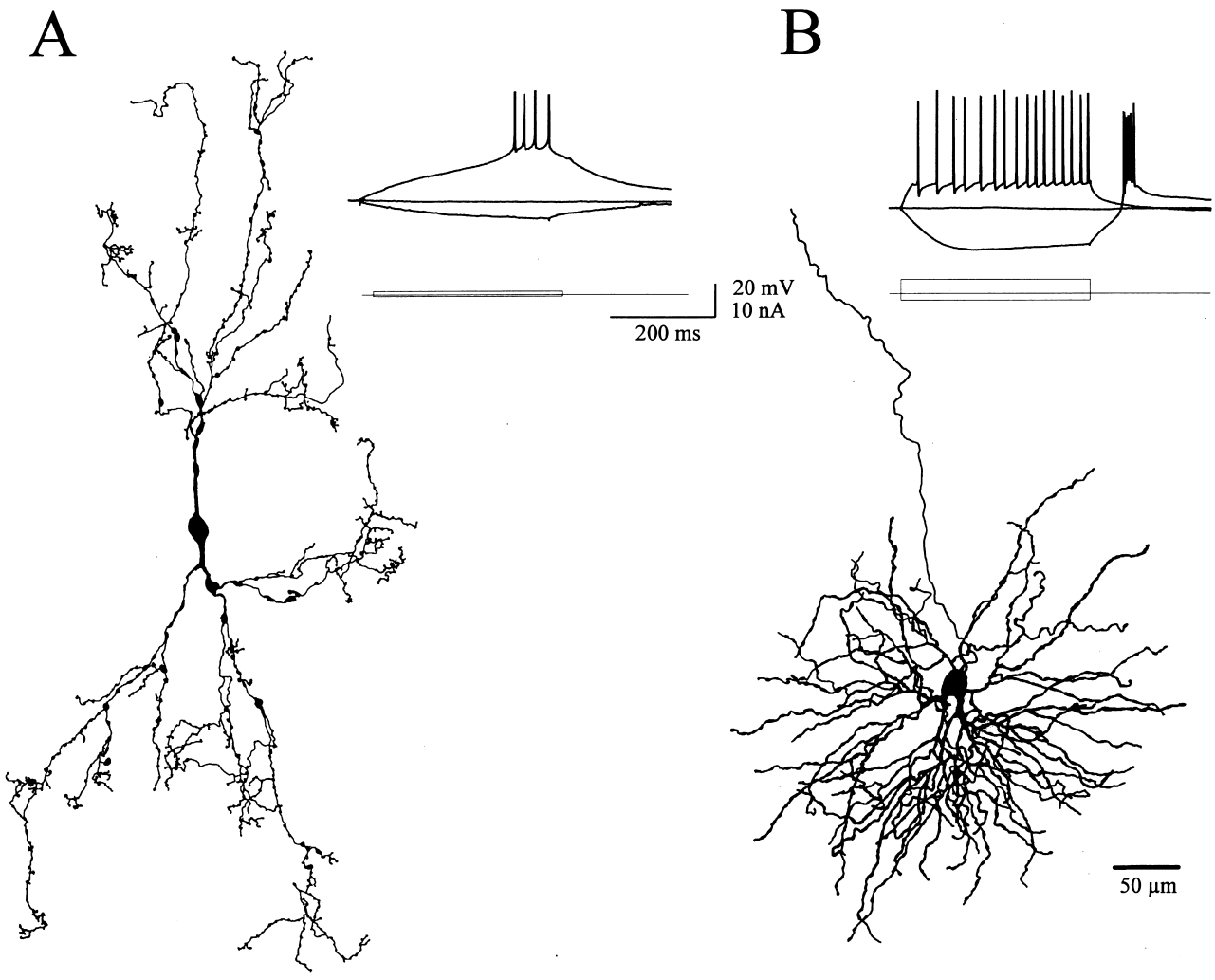

Fig. 1. Comparison of morphology and physiology of thalamic interneurons and TC cells. (A) Thalamic interneuron showing characteristic bipolar appearance and high input impedance (note size of current steps). No burst is elicited with return to resting membrane potential (RMP; −64 mV) following a hyperpolarized period. (B) The TC neuron has larger cell body and dendrites. A low-threshold spike is elicited after return to RMP (−68 mV) from a hyperpolarized potential. Action potentials truncated by sampling artifact.

Intrinsic currents underlying burst firing in interneurons

Pharmacology. The low-threshold calcium channel, I_T, underlies the low-threshold burst observed in TC and RE cells. Prior demonstration of I_T in interneurons[58] led us to consider whether I_T might also be responsible for bursts in interneurons. Blocking the fast sodium action potential with 4 μM tetrodotoxin revealed a depolarizing shoulder (Fig. 5B). Addition of 400 μM Ni^+ eliminated this transient depolarization, consistent with the pharmacological properties of I_T.

I_{CAN}, a calcium-activated non-selective cation current,[60] has been shown to contribute to the prolonged duration of bursts in RE cells.[4] Similarly, long duration bursting, as well as occasional persistence of the burst response after termination of the depolarizing current (Fig. 4B), led us to consider whether this current might also play a role in interneurons. Although no specific I_{CAN} blocker is currently available, I_{CAN} does have a characteristic pharmacological profile,[60,62,69] which we used to test for the presence of I_{CAN} in interneurons.

I_{CAN} appears to have a higher calcium sensitivity than other calcium-activated conductances, such as I_C and I_{AHP},[2,25,60,62,69] making it possible to isolate I_{CAN} from the calcium-activated potassium currents by lowering the extracellular calcium concentration. When we lowered the extracellular calcium concentration from 2 mM to 0.2–0.4 mM, action potential activity was suppressed, and a large depolarizing pulse elicited a persistent depolarizing plateau (Fig. 6B; $n=7$). This depolarized plateau was completely eliminated by substituting the residual extracellular calcium ions with 2 mM Mg^{2+} ($n=3$; not shown), consistent with mediation by a calcium-activated current.

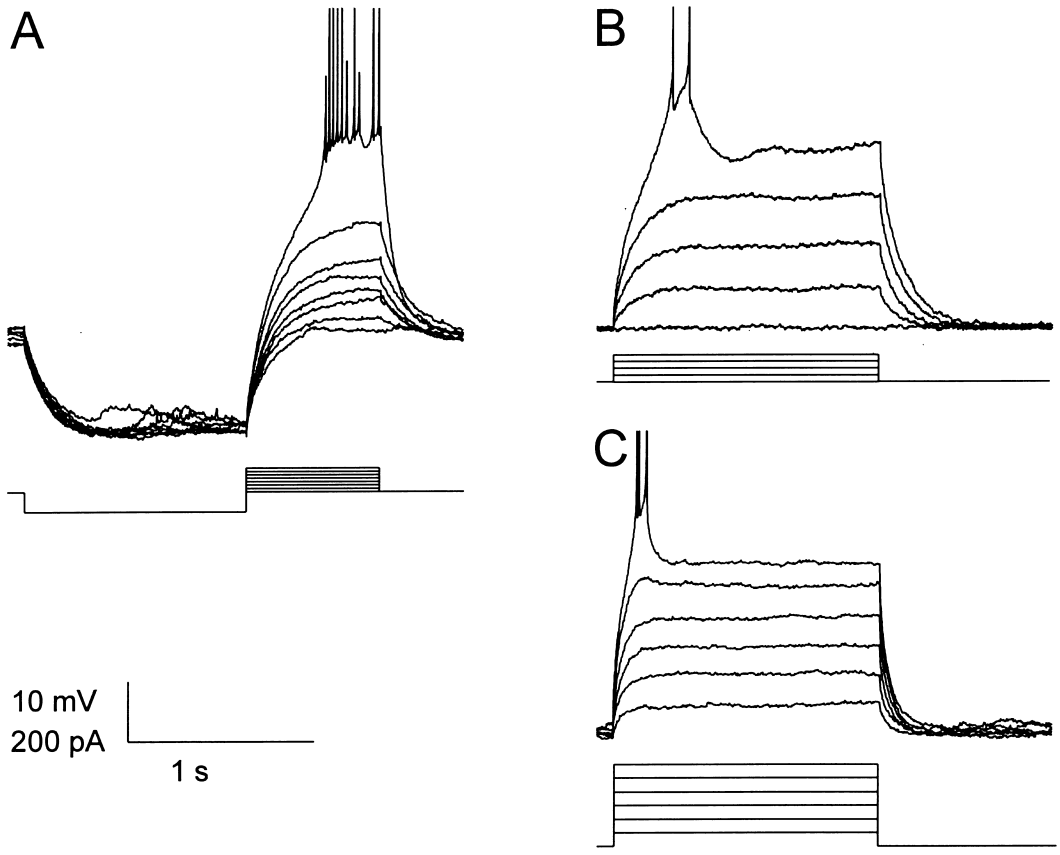

Fig. 2. Activation of burst responses in rat geniculate interneurons. (A) After a preceding hyperpolarization, a small depolarizing current pulse only induced a passive response, while a larger depolarizing current pulse evoked a burst of action potentials. The RMP of this cell was −74 mV. (B, C) In two other interneurons, the bursting responses were evoked by directly injecting large depolarizing currents when the cells were held at a slightly more hyperpolarized membrane potential. The RMPs of these cells were −64 and −67 mV, respectively. Note that action potentials in this and some of the following figures were truncated by sampling artifact or at −25 mV.

The channels supporting I_{CAN} have a large pore permeable to large cations, such as Cs^+, tetraethylammonium, $Tris^+$ and $choline^+$, but not to *N*-methyl-D-glucamine ($NMDG^+$).[4,60,87] Substituting $choline^+$ for extracellular Na^+ had little effect on the depolarized plateau ($n=2$; Fig. 6C), suggesting that the plateau current was not flowing through a persistent sodium channel. Substituting $NMDG^+$ eliminated the plateau ($n=4$; Fig. 6E). Finally, I_{CAN} described in RE cells was blocked by Sr^{2+} and enhanced by Ba^{2+}.[4] We observed similar, reversible, effects in interneurons (Fig. 6G–I; $n=2$).

Voltage-clamp. Voltage-clamp procedures were used for further study of these inward currents. The standard protocol for evaluating I_T involves stepping from a hyperpolarized holding potential to a series of depolarized potentials. When we did this ($n=6$), we observed a large, prolonged inward current (Fig. 7), instead of the transient current characteristic of I_T. We suspected that this prolonged inward current might be due to the I_{CAN} that we had observed under current clamp. Therefore, we substituted $NMDG^+$ ions for extracellular Na^+ to block this current. This eliminated the prolonged inward current and revealed a transient inward current (Fig. 7B). As reported previously,[58] the activation curve was shifted in a depolarizing direction, relative to the I_T found in TC cells, with a voltage threshold of approximately −58 mV. Time constants of activation and inactivation appeared to be consistent with previous descriptions of I_T in other thalamic cells.[14,33] Amplitude of this transient current, about one-third of the total unblocked current, had a peak of 205.4 ± 49.1 pA ($n=3$). This amplitude was somewhat greater than observed previously in dissociated cells.[58] This might be due to channels present in the slice preparation that had been removed or inactivated during cell dissociation, or could be a result of the temperature difference, due to the relatively large Q_{10} for permeability of this channel.

While the persistent current was clearly evident in all six cells tested, its time-course varied considerably, showing a slow decay in two cases (e.g., Fig. 7A) and a more rapid decay in four other cases (e.g., Fig. 7D). The reversal potential of the persistent

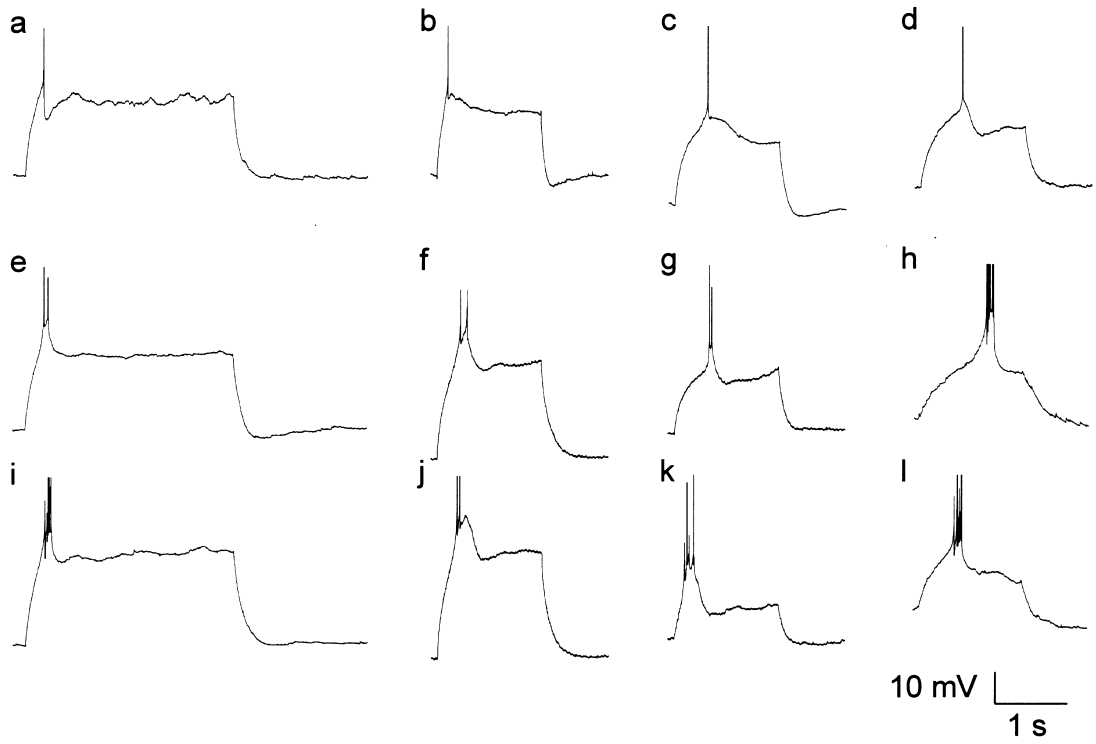

Fig. 3. Moderate variability of bursting responses in rat geniculate interneurons. Responses shown are near threshold for bursting with depolarizing current injection from resting or slightly hyperpolarized membrane potentials. The RMPs of these cells were − 66 mV (A), − 69 mV (B), 58 mV (C), 71 mV (D), − 66 mV (E), − 64 mV (F), − 67 mV (G), − 67 mV (H), − 67 mV (I), − 71 mV (J), − 73 mV (K), − 63 mV (L), − 73 mV. Statistics for multi-spike bursts: no. of spikes: 3.6 ± 1.7 (mean ± S.D.); duration of burst: 80.7 ± 33.9 ms; first interspike frequency: 29 ± 11.6 Hz. Current durations were 3.0 s (A, E, I) or 1.5 s (all others).

current, extrapolated from the current-command voltage data points, was 7.8 ± 7.3 mV ($n = 4$; e.g., Fig. 7B, inset), consistent with previous single-channel studies of I_{CAN}.[12,62,87] Ni^+ blocked both the transient and persistent currents ($n = 3$; Fig. 7E).

Computer simulation of I_T and I_{CAN}. The geniculate interneurons in our slice preparation contained conductances that were not apparent in dissociated cells, suggesting a dendritic location for these conductances. However, the unknown electrotonic distance to these conductances raises concerns about the adequacy of space clamp. Additionally, the high input resistance and long time constant associated with the whole-cell patch make temporal clamp a problem as well. These factors may introduce significant distortions in our voltage-clamp results.[16] Therefore, we used simulation to directly correlate the observed currents with activation and inactivation curves and time constants of these conductances measured previously in interneurons[58] and in other cells.[62,69]

Modeling assayed the two voltage-clamp results obtained: rapid (Fig. 7D) and slow (Fig. 7A) decay of the persistent current. Rapid decay was readily replicated in the model with the I_T and I_{CAN} models utilized (Fig. 7G). Simulated I_T blockade blocked the current (Fig. 7G, lower trace), as observed physiologically. We explored two alternative mechanisms for the slow decay case. (1) Although I_{CAN} is not believed to have significant permeability to Ca^{2+}, we found that even a very small amount of divalent permeability through this non-selective channel could give results comparable to those observed physiologically (Fig. 7H). The difference between the fast and slow decay cases could then be due to geometrical considerations that determined the exact rate of buffering for this tiny calcium current. In this case, simulated I_T blockade eliminated the current (Fig. 7H, lower trace). (2) As an alternative mechanism, we explored the possibility that a high-threshold, non-inactivating calcium current, I_L, could be responsible for the sustained component, since the terminating voltage step remained at a somewhat depolarizing voltage that would allow passage of current through this channel. However, the appearance of the trace was less satisfactorily reproduced with this model, which, with a variety of I_L density parameters, always produced a transient reduction in current at the termination of the voltage step (Fig. 7I). With this model, the I_L conductance was still apparent following simulation of Ni^+ with I_T blockade (Fig. 7I, lower trace). Therefore, we predict that these alternative models could be distinguished physiologically by using Ni^+ blockade in the slow decay case.

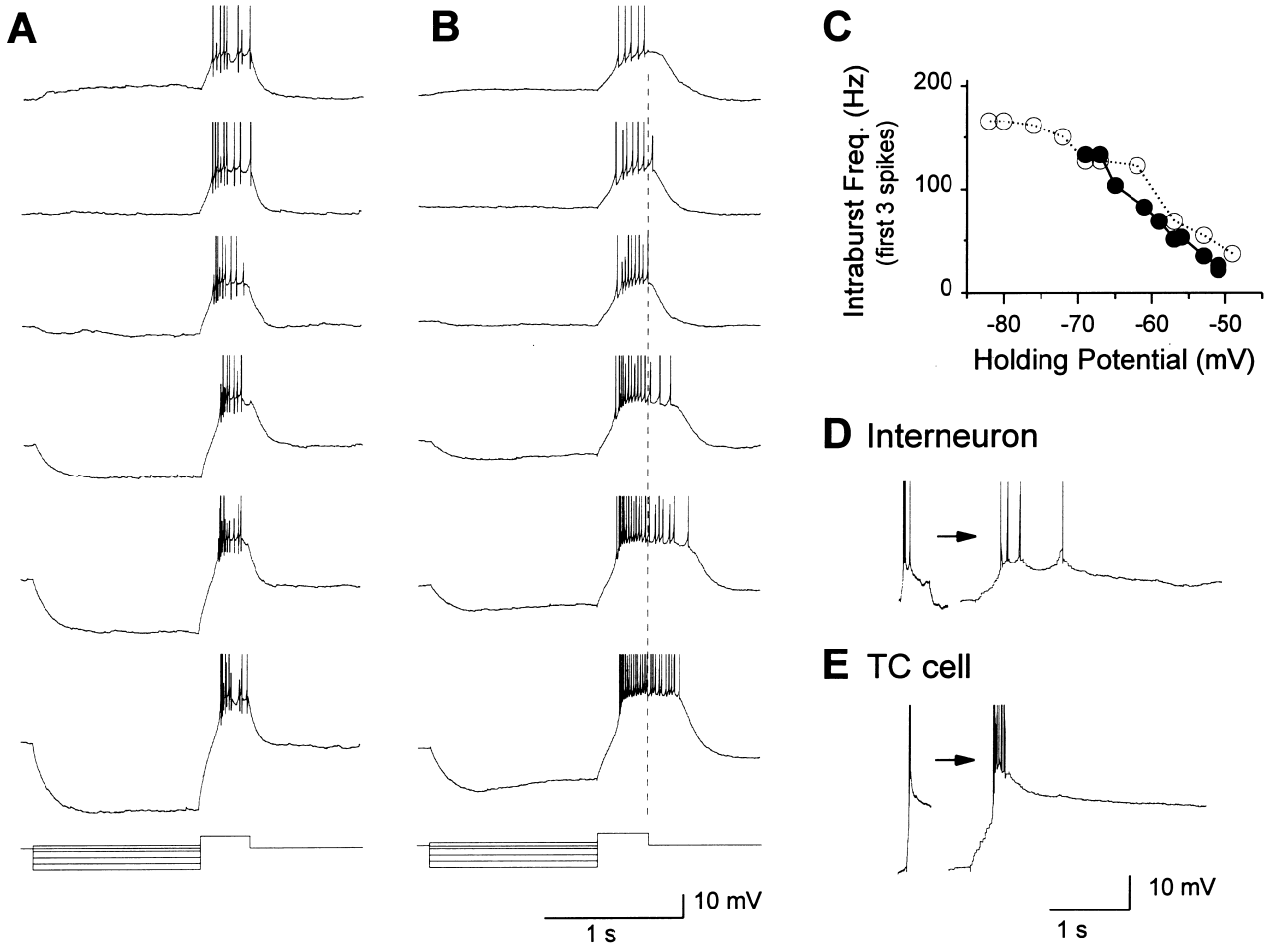

Fig. 4. Effect of prior voltage on burst responses. (A, B) Burst responses evoked by a depolarizing current injection, preceded by a hyperpolarization at different levels, in two geniculate interneurons. The RMPs of these cells were −66 and −74 mV, respectively. (C) The intraburst frequency of the first three spikes plotted against the hyperpolarization potential. (D) Burst from an interneuron expanded tenfold from Fig. 3 to show relatively slow intraburst spiking relative to E. (E) Burst in a TC cell.

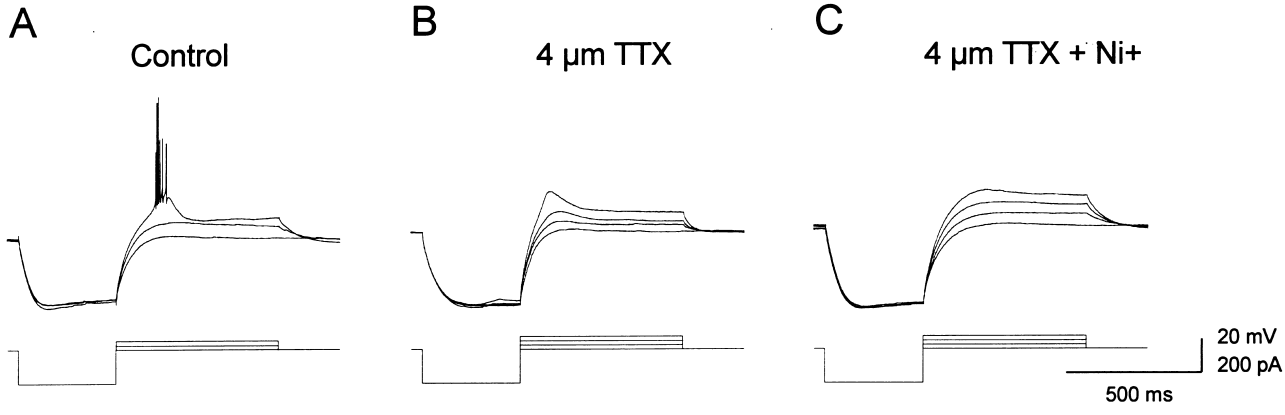

Fig. 5. Responses of a rat geniculate interneuron to current injection. (A) A small depolarizing current after a hyperpolarization elicited a bursting response in an interneuron. (B) Adding 4 mM tetrodotoxin to the bath solution revealed that a low-threshold calcium spike was underlying the burst in the cell by blocking action potentials. (C) The low-threshold calcium spike was eliminated when 400 µM Ni^+ was also included in the bath solution. The RMP of this cell was − 68 mV.

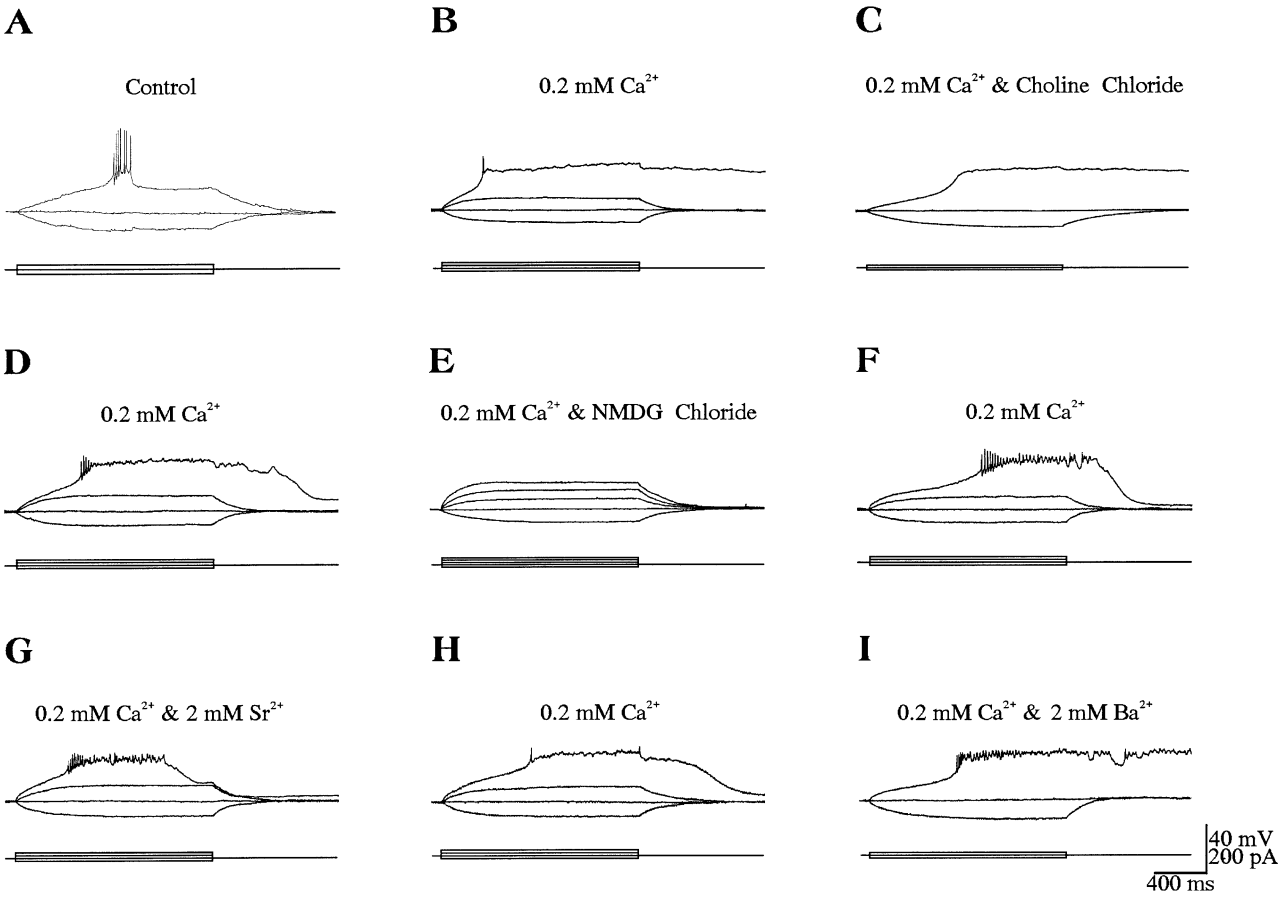

Fig. 6. The persistent depolarization has the pharmacological properties of I_{CAN}. (A) Control response, a depolarizing current injection induced a burst in an interneuron. (B) Low Ca^{2+} (0.2 mM) bath solution revealed a persistent depolarizing plateau. (C) The depolarized plateau was insensitive to the substitution of $choline^+$ for Na^+ ions, although the initial sodium spikes were blocked by this substitution. (D) The initial sodium spikes were recovered after $choline^+$ ions were washed out with solution containing a normal concentration of Na^+ ions. (E) The depolarized plateau was completely blocked by the substitution of $NMDG^+$ for Na^+ ions. (F) The depolarized plateau recovered after $NMDG^+$ ions were washed out with solution containing normal concentrations of Na^+ ions. (G) The depolarized plateau was suppressed with 2 mM of Sr^{2+} ions. (H) Suppression was removed after Sr^{2+} ions were washed out. (I) The depolarized plateau was enhanced by adding 2 mM of Ba^{2+}. RMP of this cell was −67 mV.

We then utilized the model to determine whether these conductances could explain the burst response observed in current clamp. By adjusting the density of I_T and I_{CAN}, we could produce brief bursts comparable to those seen physiologically (Fig. 8A). At higher current injections, the burst gave way to continued regular firing (Fig. 8A, lower trace), comparable to Figs 2A and 4B. Similar bursts could not be obtained in the absence of I_{CAN} (Fig. 8B). An increase in I_T density in the absence of I_{CAN} was able to produce bursting, but with an appearance far different than that seen physiologically (Fig. 8C, lower trace).

Burst responses to synaptic stimulation

The presence of burst responses with current injection led us to examine the likely physiological relevance of these bursts by determining whether they could be elicited synaptically. For this purpose, retinal axons in the optic tract were stimulated, inducing short-latency, fast-rising excitatory postsynaptic potentials (EPSPs) in the interneurons.

These EPSPs easily followed stimulating frequencies up to 100 Hz, suggesting that they were monosynaptic. Applying the non-*N*-methyl-D-aspartate (non-NMDA) receptor blocker 6,7-dinitroquinoxaline-2,3-dione (10–30 μM) to the bath solution partially blocked the EPSP ($n = 16$). The residual EPSP was eliminated by either hyperpolarizing the cell over −65 mV or by adding the NMDA receptor blocker (±)-2-amino-5-phosphonopentanoic acid (DL-APV; $n = 11$). These results confirm that retinogeniculate transmission in interneurons is mediated by both non-NMDA and NMDA receptors.[84]

Alteration of holding voltage demonstrated different portions of the postsynaptic response. When held at a depolarized membrane potential sufficient to

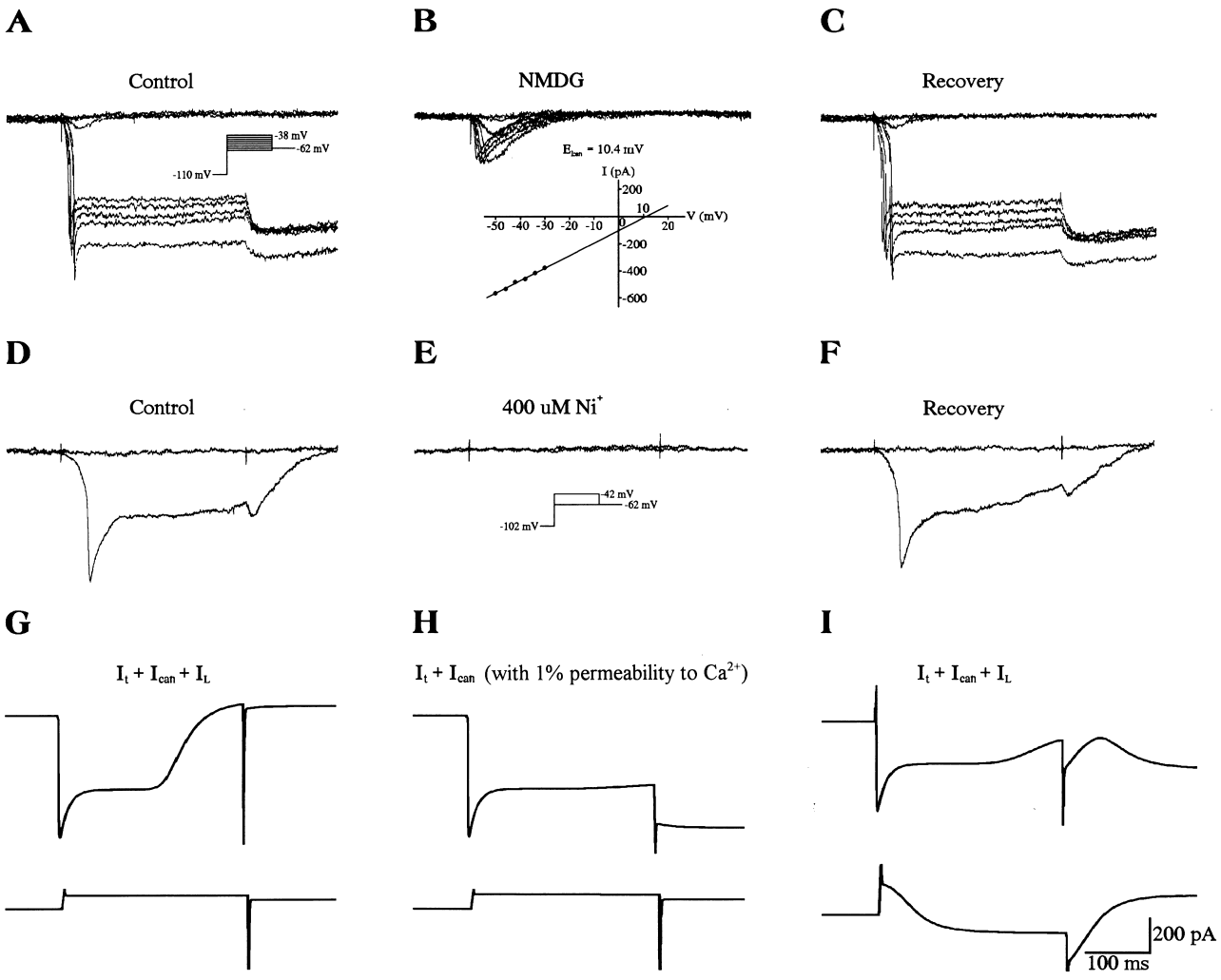

Fig. 7. I_T- and I_{CAN}-mediated inward currents in rat geniculate interneurons. (A) Depolarizing voltage steps after hyperpolarization-induced large inward current in an interneuron. (B) Substituting all extracellular Na^+ ions with $NMDG^+$ isolated the activation of I_T. (C) Normal responses were recovered after washing out $NMDG^+$. Insert in A shows the voltage protocol, applicable to A–C. Insert in B plots the current amplitude, measured right before the depolarizing voltages jump back to −62 mV, against the depolarizing command voltage. The dots were fitted by a line. The RMP of this cell was −65 mV. (D) A depolarizing voltage step induced a large inward current in another interneuron. (E) Bath application of 400 μM Ni^+ blocked the inward current, indicating that it was dependent on the activation of I_T. (F) The inward current was recovered after washing out the Ni^+ The RMP of this cell was −67 mV. (G–I) Simulations of the inward current. See text for details. Lower traces in G–I are done with I_T eliminated. Insert in E is the voltage protocol used in D–I. Scale bar below I applies to the entire figure.

inactivate the sodium channel, optic tract stimulation induced a brief EPSP, followed by a prolonged inhibitory postsynaptic potential (IPSP) of up to 450 ms duration ($n = 4$; Fig. 9A). At a less depolarized membrane potential, the IPSP was not apparent, unmasking a late depolarization and generating a single sodium action potential (Fig. 9B). At RMP or at slightly hyperpolarized membrane potentials, optic tract stimulation induced a prolonged, low-frequency burst of action potentials (Fig. 9C). The first action potentials in the burst were relatively fixed in time, while the later spikes exhibited considerable variability in latency and number.

The burst response elicited by optic tract stimulation was significantly reduced with bath application of 400 μM Ni^+ ($n = 7$; Fig. 10B) and could then be eliminated with the further addition of 100 μM DL-APV (Fig. 10C). These results could be explained by the effect of calcium influx through I_T or NMDA channels activating I_{CAN} to produce the prolonged bursting; alternatively, the prolonged bursting response may be directly mediated by NMDA current. This was further evaluated by applying DL-APV without Ni^+. Application of DL-APV alone curtailed the burst substantially (Fig. 11). Therefore, the NMDA current was directly involved in creating the prolonged burst, which could either be riding on the NMDA EPSP itself or could be due to calcium entry activating I_{CAN}.

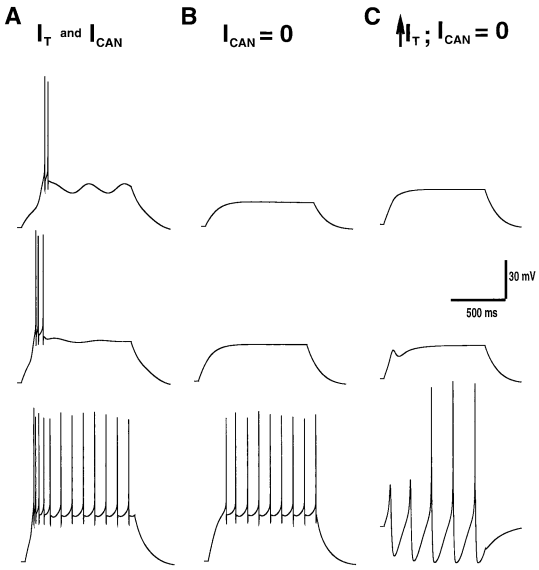

Fig. 8. Computer simulation of interneuron bursts demonstrates that the pattern of bursting observed is dependent on involvement of I_{CAN}. (A) Bursts similar to those seen physiologically obtained using the model derived from published sources and from the present voltage-clamp results. At high current injections, continued firing is seen. (From top to bottom, current injections of 20, 30 and 50 pA.) (B) With I_{CAN} removed from the simulation, the characteristic burst does not occur at any current injection strength. Current injections shown are identical to those in A. (C) Attempts to reproduce bursts utilizing higher density of I_T were unsuccessful. Single-spike bursts could be produced (lower trace), but burst appearance was entirely different from that seen in interneurons. (From top to bottom, current injections of 5, 10 and 20 pA.)

DISCUSSION

In this study, all geniculate interneurons recorded produced burst firing. The bursts were generally of prolonged duration and low frequency, distinct from the bursts found in TC cells, but somewhat similar to those of RE cells. The pattern of bursting seen was also similar to that seen in previous recordings of thalamic interneurons both *in vivo* and in *vitro*.[1,4,11,13,15,21,59,63,77,84] However, in previous *in vitro* studies, bursts were not elicited consistently.

Mechanisms of the burst

We were able to tentatively identify the conductances involved in the burst by voltage clamp. Our voltage-clamp studies were somewhat difficult to interpret, due to the extended dendritic morphology of interneurons and to our relatively high electrode series resistance. We therefore performed simulations using these voltage-clamp data. The simulations served as a test of internal consistency of our data, demonstrating that our interpretation of the voltage clamp is consistent with the current-clamp findings.

It is now well established that dendrites are endowed with a wide range of voltage-gated channels.[31,65,73,78] Dendritic channels have also been demonstrated in thalamic interneurons.[10] This may be expected to produce difficulties with maintaining adequate spatial control of voltage, despite the apparent compactness of the interneuron with its high membrane resistance. Unfortunately, the difficulty of obtaining interneurons lead us to utilize electrodes with relatively high series resistance values, which could increase somatic voltage errors. It is therefore possible that the persistent current seen under voltage clamp in Fig. 7 might be partially due to poor spatial control of distant regenerative inward current. However, our ability to replicate similar curves with the computer model (Fig. 7G–I) suggests that this possible artifact is not the major determinant of the current behavior. We did not find it necessary to actually include dendritic channels in the model, since the interneuron is compact enough that changes in channel placement from soma to proximal dendrite did not alter the simulations significantly.

Like the LTS originally studied in TC cells, the bursts of LGN interneurons depended on I_T. Like the burst response of RE cells, the interneuron burst depended not only on I_T, but on I_{CAN} as well. A major difference from burst characteristics of these two cell types can be traced to differences in the activation and inactivation curves of I_T, described previously by Pape *et al.*[58] and confirmed in this study. Both curves are shifted in a depolarizing direction relative to the I_T described in other neurons. The shift in inactivation curve reduces the need for a preceding hyperpolarization, since there is significant deinactivation at RMP. The shift in activation curve necessitates a depolarizing boost in order to produce activation. This difference suggested the activating protocol that was used in this study, and partially explains the difference from previous *in vitro* studies, discussed further below.

The duration of the interneuron burst, though highly variable, is considerably longer than that seen in TC cells. This prolongation is consistent with a role for I_{CAN}, comparable to that seen in RE cells. Ca^{2+} influx through I_T serves to activate this calcium-sensitive channel. Continued inward current through this channel serves to maintain a depolarized plateau, which may or may not support continued sodium spiking, depending on the precise relationship between this depolarization and sodium spike threshold. Computer modeling of the burst illustrated this relationship, showing that increase in the depolarizing pulse could prolong the duration of spiking (Fig. 8A, top to bottom). Computer modeling also demonstrated that I_{CAN} was required to produce the burst morphology observed (Fig. 8B). Increased levels of I_T could not produce similar bursts, but would instead produce brief bursts with large voltage excursions more similar to those seen in TC cells, although shifted in a depolarized direction (Fig. 8C).

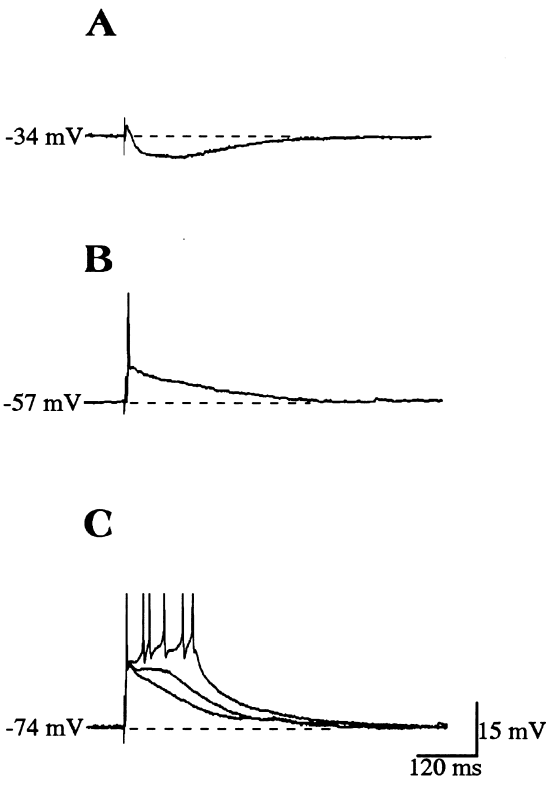

Fig. 9. Responses of a rat geniculate interneuron to synaptic stimulation: effect of holding potential. (A) Stimulation of the optic tract induced an EPSP followed by an IPSP when the cell was held at −34 mV. (B) Stimulation of the optic tract induced a supra-threshold EPSP when the interneuron was held at −57 mV. (C) Three traces with cell held at −74 mV. Stimulation of the optic tract induced EPSPs, and sometimes a low-threshold calcium spike and a burst of action potentials. The RMP of this cell was −71 mV.

Differences from previous studies

Our results differ from those of previous *in vitro* studies in that we observed burst responses in all interneurons tested, whereas bursts were found inconsistently in previous studies.[52,59,84] Technical and procedural differences between previous work and the present study account for these differences. In order to consistently obtain bursts, it was necessary in most interneurons to give a depolarizing boost. This boost is not needed in other neurons showing I_T-dependent bursts, such as TC cells, and depolarizing boosts were not used in previous studies of interneurons. As noted above, this result is consistent with the voltage-clamp findings of Pape *et al.*,[58] showing a depolarizing shift in activation and inactivation curves.

A further difference with most previous studies is our use of the whole-cell patch technique, instead of sharp-electrode impalement. The loss of input resistance associated with impalement will tend to produce shunting and reduce bursting.[74] With the whole-cell technique, we obtained much higher input resistance recordings. This would tend to favor the expression of regenerative currents, such as I_T, which could otherwise be shunted by the impalement-associated leak. In addition, the higher input resistance allows electrotonic integration with the dendrites of the interneuron. This is important in interneurons because of their large dendritic extent (see below) and because a significant amount of T channel is found in the dendrites.[10] The higher input resistance would allow a greater contribution from these dendritic T channels.

Even with use of a depolarizing boost and with the whole-cell technique, bursts were not observed in dissociated geniculate interneurons.[58] In that study, the researchers concluded that a transient K^+ current, I_A, prevented burst firing. We tested this hypothesis in our computer model and were able to show that I_A could prevent burst firing, as other K^+ currents with different dynamics could. However, we believe that additional factors also contributed to the lack of burst firing in the previous study. Most notably, dendrites are typically removed in dissociated neurons. This would eliminate the contribution of the significant number of I_T channels localized in interneuron dendrites.[10]

Our voltage-clamp results were also consistent with substantial dendritic localization of I_T, showing a peak conductance twice that seen with dissociated neurons in the same previous study.[58] This peak conductance difference could, however, be alternatively explained by the relatively high Q_{10} for I_T channel permeability, given the temperature difference between the two studies. The higher temperature of the present study (34°C instead of room temperature) would of course also produce significantly faster I_T activation,[14] further encouraging burst formation.

Another difference with this previous dissociated cell study lies in our description of I_{CAN}, a current not identified in the dissociated interneurons. I_{CAN} was found to disappear from RE cells following dissociation.[4,34] This observation, not fully explained, might also suggest that I_{CAN} is present in considerable amounts in the dendrites. Were this the case, it raises the intriguing possibility that the I_T–I_{CAN} linkage required in the computer model might be strengthened due to the restricted diffusion volume for Ca^{2+} available in the dendrites.

Synaptic stimulation

Optic tract stimulation evoked an EPSP/IPSP sequence in geniculate interneurons. The excitatory transmission was mediated by both non-NMDA and NMDA conductances, consistent with previous studies.[84] The shape of the postsynaptic response depended on the holding potential of the interneuron. The characteristic burst was seen with optic tract stimulation with the cell initially maintained at a hyperpolarized membrane potential. This is consistent with a role for the non-NMDA

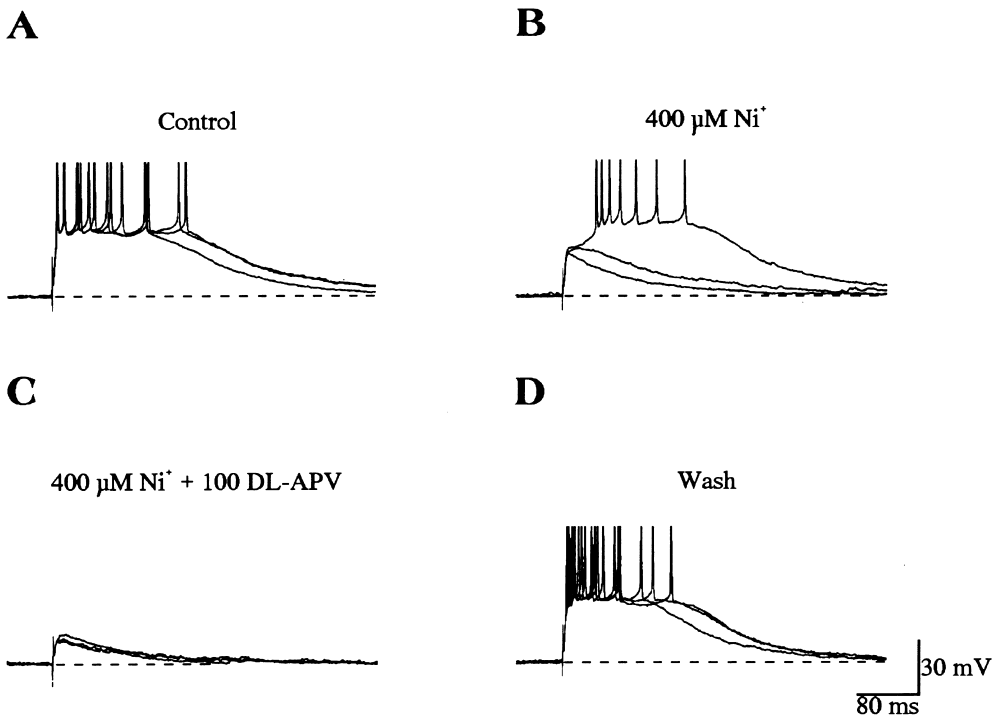

Fig. 10. Responses of a rat geniculate interneuron to synaptic stimulation. (A) Stimulation of the optic tract induced bursting responses when the cell was held at −79 mV. (B) Bath application of Ni^+ decreased the amplitude of EPSPs and the possibility of firing a burst of action potentials. However, a bursting response with a prolonged latency did occur occasionally. (C) Addition of DL-APV further decreased the EPSPs and completely blocked the bursting response. (D) After washing out the Ni^+ and DL-APV, the bursting responses were completely recovered. RMP was −70 mV.

receptor-mediated EPSP in initiating the burst by activation of I_T. The calcium influx would then activate I_{CAN}, according to the model detailed above. The voltage increase would also permit further current flow through NMDA receptor channels.

In contrast, starting from depolarized membrane potentials, I_T is relatively inactivated, diminishing the burst. In this setting, a pronounced IPSP is revealed. The subsequent IPSP must come from activation of other interneurons, because the other likely source of inhibition, the RE, was not present in the slice. This finding agrees with those of Williams *et al.*,[85] and is consistent with anatomical evidence for mutual inhibitory connections between interneurons.[20,44,61,86] The prolonged duration of the IPSP is consistent with previous studies that have demonstrated primarily $GABA_A$ receptors on these cells, with some evidence of a $GABA_B$ effect as well.[59,84] The prolonged IPSP could either be due to these $GABA_B$ receptors or could be evidence of presynaptic burst firing in other interneurons producing summation, which appears as a single IPSP due to low-pass filtering in the dendrites.

Dendritic signal integration

In our whole-cell preparation, LGN interneurons had input resistances and time constants roughly five times greater than those reported in previous studies using sharp electrodes.[52,59,84] This has implications for how interneurons integrate electrical signals generated at different locations in the dendritic tree and for how widely this information is disseminated via the various presynaptic specializations of a single interneuron.

The role of interneuron dendrites and their interaction with other dendrites and the soma were explored by Bloomfield and Sherman in a modeling study.[8] They concluded that individual dendritic trees of interneurons were electrotonically isolated from each other and from the soma. However, Bloomfield and Sherman utilized data from recordings with sharp electrodes. Because of the leak associated with the impalement, they used a far lower value for input impedance, and hence for membrane resistance, than we have found. The higher membrane resistance that we find implies a more electrotonically compact cell than predicted by the old model. This agrees with revised models of other cell types using the whole-cell patch technique.[9]

Input resistance and length constant are not static properties. They can be modified by neuromodulators that alter intrinsic potassium conductances or by repetitive synaptic input resulting in tonically active synaptic conductances, whether classical shunting $GABA_A$ or mixed excitatory and inhibitory activation.[6] In interneurons, acetylcholine can reduce input resistance via muscarinic and nicotinic

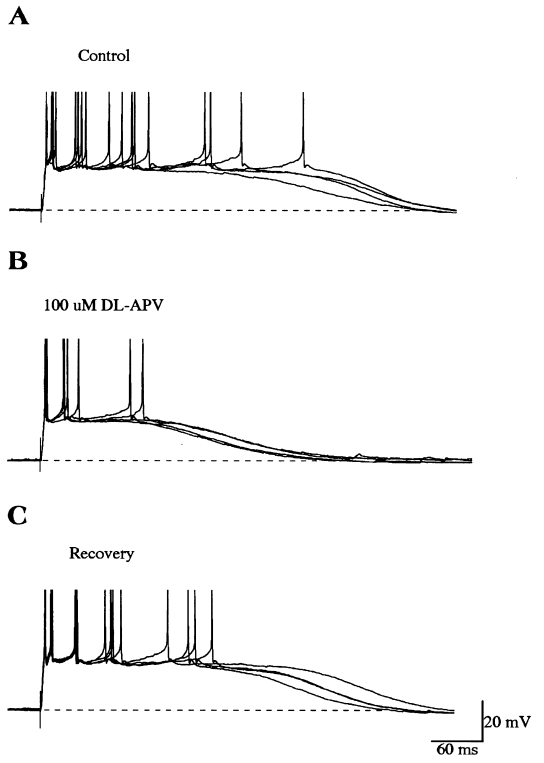

Fig. 11. Responses of a rat geniculate interneuron to synaptic stimulation. (A) Stimulation of the optic tract induced bursting responses when the cell was held at − 71 mV. (B) The bursting responses were curtailed by bath application of DL-APV. (C) After washing out the DL-APV, the prolonged bursting responses recovered. RMP was − 67 mV.

receptors.[52,90] This raises the possibility that interneurons may alternate between compact and extended states, with respective high and low cooperativity between distant dendritic output sites. This will affect how input from cortex, RE cells and other interneurons is processed by the cell, and what output reaches other interneurons and TC cells via dendrodendritic synapses. The contribution of dendritic T channels to burst behavior will also depend on the electrotonic proximity of these channels to other channels involved in the burst.

Functional considerations

Inhibitory mechanisms have been implicated both in the processing and transmission of sensory information, and in the generation of slow electroencephalogram oscillations during sleep. Although the details of inhibitory function for each of these thalamic functions remain unclear, the apparently linear response of interneurons has led to the notion that their contribution will be relatively straightforward. The presence of a robust, voltage-dependent burst in thalamic interneurons suggests that the contribution of these cells to thalamic function will be more complex than previously thought.

Our results suggest that interneuron responses to retinal input may be state dependent, as they are in TC cells: a single spike with the interneuron depolarized (Fig. 9B) and a burst of action potentials with a preceding hyperpolarization (Fig. 9C). In TC cells, two firing modes are clearly correlated with behavioral state.[30,50,55,75] During sleep, TC cells are relatively hyperpolarized and generate bursts of action potentials due to the deinactivation of I_T. This burst mode of firing is associated with the generation of low-frequency delta and spindle oscillations that are seen in the electroencephalogram. In contrast, during the waking state, TC cells are relatively depolarized and exhibit tonic (single-spike) firing patterns that more linearly reflect incoming sensory signals.[24,45] Burst responses in TC cells are observed under certain conditions in the waking state.[24] In this setting, it has been suggested that they non-linearly amplify salient sensory information for transmission to the cortex.[24,67]

An early *in vivo* study suggested that the response of thalamic interneurons also varied depending on behavioral state,[63] implying different, state-dependent roles of the inhibitory actions of interneurons. Bursts of action potentials in thalamic interneurons might be expected to generate larger and longer inhibitions in TC cells by non-linear activation of $GABA_B$ receptors.[18,35,36] Such large inhibitions would amplify the inhibitory aspects of the salient sensory signals, while giving poor temporal resolution due to their slow time-course. In the TC cells, this inhibitory augmentation would subsequently be expressed as an amplification of the LTS. The augmentation would be particularly relevant during the slow oscillations of sleep. Because interneurons are connected with the other cell types involved in slow thalamic oscillations, they could serve to help synchronize these oscillations[58] through their bursting.[46,47] Furthermore, we have found evidence that interneurons can also produce intrinsically generated burst oscillations,[91] suggesting an even more prominent role in slow oscillations.

It is also likely that burst behavior in interneurons plays a role in sensory processing. For example, interneuron bursts may contribute to the 'lagged' visual responses seen in some TC cells of the LGN.[37,49] In response to sudden onset of a visual stimulus, lagged TC cells exhibit an initial 65–200 ms reduction in baseline firing before responding at elevated levels. This lagged response is not observed in the presynaptic retinal ganglion cells recorded simultaneously,[49] suggesting a geniculate origin for the lagged property. In fact, Humphrey and Weller[37] argued that inhibition from interneurons plays the primary role in the lagged response. This hypothesis is supported by results that show that the inhibitory 'dip' is sensitive to the iontophoretic application of bicuculline in the

LGN.[27,51] Prolonged bursts in interneurons could be responsible for such an initial long inhibition in the lagged cells. The lagged property can be altered by activation of cholinergic cells in the brainstem, suggesting that the degree of lag may be state dependent.[38,80] This could be explained, in part, by the variation in burst response with polarization that we observed.

CONCLUSION

Inhibitory mechanisms play an important role in thalamic function, due in part to the existence of low-threshold bursting mechanisms in the other major cell types of the thalamus. The presence of similar bursting mechanisms in the inhibitory interneurons suggests additional complexity for the functional thalamic circuit. Although the depolarized shift in the threshold for activation of low-threshold bursts in interneurons makes them somewhat less dependent on hyperpolarization preceding a burst, the requirement for a period of preceding quiescence is still there. This requirement will doubtless have significance for patterns of oscillation within the network as a whole. The importance of thalamic oscillations in sleep and epilepsy underlines the importance of further understanding these highly non-linear responses.

REFERENCES

1. Ahlsén G., Lindström S. and Lo F.-S. (1984) Inhibition from the brain stem of inhibitory interneurons of the cat's dorsal lateral geniculate nucleus. *J. Physiol., Lond.* **347,** 593–609.
2. Art J. J., Wu Y.-C. and Fettiplace R. (1995) The calcium-activated potassium channels of turtle hair cells. *J. gen. Physiol.* **105,** 49–72.
3. Avanzini G., de Curtis M., Panzica F. and Spreafico R. (1989) Intrinsic properties of nucleus reticularis thalami neurones of the rat studied *in vitro*. *J. Physiol., Lond.* **416,** 111–122.
4. Bal T. and McCormick D. A. (1993) Mechanisms of oscillatory activity in guinea pig nucleus reticularis thalami *in vitro*: a mammalian pacemaker. *J. Physiol., Lond.* **468,** 669–691.
5. Bal T., von Krosigk M. and McCormick D. A. (1995) Synaptic and membrane mechanisms underlying synchronized oscillation in the ferret LGNd *in vitro*. *J. Physiol., Lond.* **483,** 641–663.
6. Bernander O., Douglas R. J., Martin K. A. C. and Koch C. (1991) Synaptic background activity influences spatio-temporal integration in single pyramidal cells. *Proc. natn. Acad. Sci. U.S.A.* **88,** 11,569–11,573.
7. Blanton M. G., Turco J. J. and Kriegstein A. R. (1989) Whole cell recording from neurons in slices of reptilian and mammalian cerebral cortex. *J. Neurosci. Meth.* **30,** 203–210.
8. Bloomfield S. and Sherman S. (1989) Dendritic current flow in relay cells and interneurons of the cat's lateral geniculate nucleus. *Proc. natn. Acad. Sci. U.S.A.* **86,** 3911–3914.
9. Bloomfield S. A. (1992) Relationship between receptive and dendritic field size of amacrine cells in the rabbit retina. *J. Neurophysiol.* **68,** 711–725.
10. Budde T., Munsch T. and Pape H. C. (1996) Different spatial profile of intracellular calcium transients and fluorescent dihydropyridine binding in relay cells and local interneurons from the rat dorsal lateral geniculate nucleus. *Soc. Neurosci. Abstr.* **22,** 495.13.
11. Burke W. and Sefton J. (1966) Discharge patterns of principal cells and interneurons in lateral geniculate nucleus of rat. *J. Physiol., Lond.* **187,** 201–212.
12. Colquhoun D., Neher E., Reuter H. and Stevens C. F. (1981) Inward current channels activated by intracellular Ca^{2+} in cultured cardiac cells. *Nature* **294,** 752–754.
13. Contreras D., Dossi R. C. and Steriade M. (1993) Electrophysiological properties of cat reticular thalamic neurones *in vivo*. *J. Physiol., Lond.* **470,** 273–294.
14. Coulter D. A., Huguenard J. R. and Prince D. A. (1989) Calcium currents in rat thalamocortical relay neurones: kinetic properties of the transient low-threshold current. *J. Physiol., Lond.* **414,** 587–604.
15. Deschênes M., Paradis M., Roy J. P. and Steriade M. (1984) Electrophysiology of neurons of lateral thalamic nuclei in cat: resting properties and burst discharges. *J. Neurophysiol.* **51,** 1196–1219.
16. Destexhe A., Contreras D., Steriade M., Sejnowski T. J. and Huguenard J. R. (1996) *In vivo*, *in vitro* and computational analysis of dendritic calcium currents in thalamic reticular neurons. *J. Neurosci.* **16,** 169–185.
17. Destexhe A., Mainen Z. F. and Sejnowski T. J. (1994) Synthesis of models for excitable membranes, synaptic transmission and neuromodulation using a common kinetic formalism. *J. comput. Neurosci.* **1,** 195–230.
18. Destexhe A. and Sejnowski T. J. (1995) G protein activation kinetics and spillover of gamma-aminobutyric acid may account for differences between inhibitory responses in the hippocampus and thalamus. *Proc. natn. Acad. Sci. U.S.A.* **92,** 9515–9519.
19. Edwards F. A., Konnerth A., Sakmann B. and Takahashi T. (1989) A thin slice preparation for patch clamp recordings from neurones of the mammalian central nervous system. *Pflügers Arch.* **414,** 600–612.
20. Famiglietti E. V. and Kolb H. (1976) Structural basis of on and off center responses in retinal ganglion cells. *Science* **194,** 193–195.
21. Fukuda Y. and Iwama K. (1970) Inhibition of lateral geniculate body interneurons by activation of the reticular formation. *Brain Res.* **18,** 548–551.
22. Gabbott P. L., Somogyi J., Stewart M. G. and Hamori J. (1986) A quantitative investigation of the neuronal composition of the rat dorsal lateral geniculate nucleus using GABA-immunocytochemistry. *Neuroscience* **19,** 101–111.
23. Grossman A., Lieberman A. R. and Webster K. E. (1973) A Golgi study of the rat dorsal lateral geniculate nucleus. *J. comp. Neurol.* **150,** 441–466.
24. Guido W. and Weyand T. (1992) Burst responses in thalamic relay cells of the awake behaving cat. *J. Neurophysiol.* **74,** 1782–1786.
25. Gurney A. M., Tsien R. Y. and Lester H. A. (1987) Activation of a potassium current by rapid photochemically generated step increases of intracellular calcium in rat sympathetic neurons. *Proc. natn. Acad. Sci. U.S.A.* **84,** 3496–3500.

26. Hamill O. P., Marty A., Neher E., Sakmann B. and Sigworth F. J. (1981) Improved patch-clamp techniques for high-resolution current recording from cells and cell-free membrane patches. *Pflügers Arch.* **391,** 85–100.
27. Heggelund P. and Hartveit E. (1990) Neurotransmitter receptors mediating excitatory input to cells in the cat dorsal lateral geniculate nucleus. I. Lagged cells. *J. Neurophysiol.* **63,** 1347–1360.
28. Helmchen F., Imoto K. and Sakmann B. (1996) Ca^{2+} buffering and action potential-evoked Ca^{2+} signaling in dendrites of pyramidal neurons. *Biophys. J.* **70,** 1069–1081.
29. Hines M. (1993) NEURON—a program for simulation of nerve equations. In *Neural Systems: Analysis and Modeling* (ed. Eeckman F.), pp. 127–136. Kluwer, Norwell, MA.
30. Hirsch J. C., Fourment A. and Marc M. E. (1983) Sleep-related variations of membrane potential in the lateral geniculate body relay neurons of the cat. *Brain Res.* **259,** 308–312.
31. Hoffman D. A., Magee J. C., Colbert C. M. and Johnston D. (1997) K^+ channel regulation of signal propagation in dendrites of hippocampal pyramidal neurons. *Nature* **387,** 869–875.
32. Horikawa K. and Armstrong W. E. (1988) A versatile means of intracellular labeling: injection of biocytin and its detection with avidin conjugates. *J. Neurosci. Meth.* **25,** 1–11.
33. Huguenard J. R. and Prince D. A. (1991) An unconventional transient Ca^{2+} current in GABAergic neurons of rat thalamic reticular nucleus. *Soc. Neurosci. Abstr.* **17,** 142.9.
34. Huguenard J. R. and Prince D. A. (1992) A novel T-type current underlies prolonged calcium-dependent burst firing in GABAergic neurons of rat thalamic reticular nucleus. *J. Neurosci.* **12,** 3804–3817.
35. Huguenard J. R. and Prince D. A. (1994) Clonazepam suppresses $GABA_B$-mediated inhibition in thalamic relay neurons through effects in nucleus reticularis. *J. Neurophysiol.* **71,** 2576–2581.
36. Huguenard J. R. and Prince D. A. (1994) Intrathalamic rhythmicity studied *in vitro*: nominal T-current modulation causes robust antioscillatory effects. *J. Neurosci.* **14,** 5485–5502.
37. Humphrey A. L. and Weller R. E. (1988) Functional distinct groups of x-cells in the lateral geniculate nucleus of the cat. *J. comp. Neurol.* **268,** 429–447.
38. Humphrey A. L. and Saul A. B. (1992) Action of brain stem reticular afferents on lagged and nonlagged cells in the cat lateral geniculate nucleus. *J. Neurophysiol.* **68,** 673–691.
39. Jahnsen H. and Llinás R. (1984) Electrophysiological properties of guinea pig thalamic neurones: an *in vitro* study. *J. Physiol., Lond.* **349,** 205–226.
40. Jahnsen H. and Llinás R. (1984) Ionic basis for the electroresponsiveness and oscillatory properties of guinea-pig thalamic neurons *in vitro*. *J. Physiol., Lond.* **349,** 227–247.
41. Jones E. G. (1985) *The Thalamus.* Plenum, New York.
42. Kay A. R. and Wong R. K. S. (1987) Calcium current activation kinetics in isolated pyramidal neurones of the CA1 region of the mature guinea-pig hippocampus. *J. Physiol., Lond.* **392,** 603–616.
43. Leresche N., Lightowler S., Soltesz I., Jassik-Gerschenfeld D. and Crunelli V. (1991) Low-frequency oscillatory activities intrinsic to rat and cat thalamocortical cells. *J. Physiol., Lond.* **441,** 155–174.
44. Lieberman A. R. and Webster K. E. (1974) Aspects of the synaptic organization of intrinsic neurons in the dorsal lateral geniculate nucleus: an ultrastructure study of the normal and of the experimentally deafferented nucleus in the rat. *J. Neurocytol.* **3,** 677–710.
45. Lu S. M., Guido W. and Sherman S. M. (1992) Effects of membrane voltage on receptive field properties of lateral geniculate neurons in the cat: contributions of the low-threshold Ca^{2+} conductance. *J. Neurophysiol.* **68,** 2185–2198.
46. Lytton W. W., Destexhe A. and Sejnowski T. J. (1996) Control of slow oscillations in the thalamocortical neuron: a computer model. *Neuroscience* **70,** 673–684.
47. Lytton W. W. and Sejnowski T. J. (1991) Inhibitory interneurons may help synchronize oscillations in cortical pyramidal neurons. *J. Neurophysiol.* **66,** 1059–1079.
48. Markram H., Helm P. J. and Sakmann B. (1995) Dendritic calcium transients evoked by single back-propagating action potentials in rat neocortical pyramidal neurons. *J. Physiol., Lond.* **485,** 1–20.
49. Mastronarde D. N. (1987) Two classes of single-input X-cells in cat lateral geniculate nucleus: II retinal inputs and the generation of receptive-field properties. *J. Neurophysiol.* **57,** 381–413.
50. McCarley R. W., Benoit O. and Barrionuevo G. (1983) Lateral geniculate nucleus unitary discharge in sleep and waking: state- and rate-specific aspects. *J. Neurophysiol.* **50,** 798–818.
51. McCormick D. A. (1991) Functional properties of a slowly inactivating potassium current in guinea pig dorsal lateral geniculate relay neurons. *J. Neurophysiol.* **66,** 1176–1189.
52. McCormick D. A. and Pape H. C. (1988) Acetylcholine inhibits identified interneurons in the cat lateral geniculate nucleus. *Nature* **334,** 246–248.
53. McCormick D. A. and Pape H. C. (1990) Noradrenergic and serotonergic modulation of a hyperpolarization-activated cation current in thalamic relay neurones. *J. Physiol., Lond.* **431,** 319–342.
54. McCormick D. A. and Pape H. C. (1990) Properties of a hyperpolarization-activated cation current and its role in rhythmic oscillation in thalamic relay neurones. *J. Physiol., Lond.* **431,** 291–318.
55. McCormick D. A. and von Krosigk M. (1992) Corticothalamic activation modulates thalamic firing through glutamate metabotropic receptors. *Proc. natn. Acad. Sci. U.S.A.* **89,** 2774–2778.
56. Norton T. T. and Gudwin D. W. (1992) Inhibitory GABAergic control of visual signals at the lateral geniculate nucleus. *Prog. Brain Res.* **90,** 192–217.
57. O'Hara P. T., Lieberman A. R., Hunt S. P. and Wu J. Y. (1983) Neural elements containing glutamic acid decarboxylase (GAD) in the dorsal lateral geniculate nucleus of the rat; immunohistochemical studies by light and electron microscopy. *Neuroscience* **8,** 189–211.
58. Pape H. C., Budde T., Mager R. and Kisvarday Z. F. (1994) Prevention of Ca^{2+}-mediated action potentials in GABAergic local circuit neurones of rat thalamus by a transient K^+ current. *J. Physiol., Lond.* **478,** 403–422.
59. Pape H. C. and McCormick D. A. (1995) Electrophysiological and pharmacological properties of interneurons in the cat dorsal lateral geniculate nucleus. *Neuroscience* **68,** 1105–1125.
60. Partridge L. and Swandulla D. (1988) Calcium-activated non-specific cation channels. *Trends Neurosci.* **11,** 69–72.
61. Pasik P., Pasik T. and Hamori J. (1976) Synapses between interneurons in the lateral geniculate nucleus of monkeys. *Expl Brain Res.* **25,** 1–13.
62. Razani-Boroujerdi S. and Partridge L. D. (1993) Activation and modulation of calcium-activated non-selective cation channels

from embryonic chick sensory neurons. *Brain Res.* **623,** 195–200.
63. Sakakura H. (1968) Spontaneous and evoked unitary activities of cat lateral geniculate neurons in sleep and wakefulness. *Jap. J. Physiol.* **18,** 23–42.
64. Schiller J., Helmchen F. and Sakmann B. (1995) Spatial profile of dendritic calcium transient evoked by action potentials in rat neocortical pyramidal neurons. *J. Physiol., Lond.* **487,** 583–600.
65. Schwindt P. C. and Crill W. E. (1997) Local and propagated dendritic action potentials evoked by glutamate iontophoresis on rat neocortical pyramidal neurons. *J. Neurophysiol.* **77,** 2466–2483.
66. Sherman S. and Koch C. (1986) The control of retinogeniculate transmission in the mammalian lateral geniculate nucleus. *Expl Brain Res.* **63,** 1–20.
67. Sherman S. M. (1996) Dual response modes in lateral geniculate neurons: mechanisms and functions. *Visual Neurosci.* **13,** 205–213.
68. Sherman S. M. and Guillery R. W. (1996) Functional organization of thalamocortical relays. *J. Neurophysiol.* **76,** 1367–1395.
69. Simonneau M., Distasi C., Tauc L. and Barbin G. (1987) Potassium channels in mouse neonate dorsal root ganglion cells: a patch-clamp study. *Brain Res.* **412,** 224–232.
70. Soltesz I. and Crunelli V. (1992) $GABA_A$ and pre- and post-synaptic $GABA_B$ receptor-mediated responses in the lateral geniculate nucleus. *Prog. Brain Res.* **90,** 151–169.
71. Soltesz I., Lightowler S., Leresche N., Jassik-Gerschenfeld D., Pollard C. E. and Crunelli V. (1991) Two inward currents and the transformation of low-frequency oscillations of rat and cat thalamocortical cells. *J. Physiol., Lond.* **44,** 175–197.
72. Spiegel E. A. and Wycis H. T. (1950) Thalamic recording in man: special reference to seizure discharges. *Electroenceph. clin. Neurophysiol.* **2,** 23–27.
73. Spruston N., Schiller Y., Stuart G. and Sakmann B. (1995) Activity-dependent action potential invasion and calcium influx into hippocampal CA1 dendrite. *Science* **8,** 297–300.
74. Staley K. J., Otis T. S. and Mody I. (1992) Membrane properties of dentate gyrus granule cells—comparison of sharp microelectrode and whole-cell recordings. *J. Neurophysiol.* **67,** 1346–1358.
75. Steriade M. and Llinás R. R. (1988) The functional states of the thalamus and the associated neuronal interplay. *Physiol. Rev.* **68,** 649–742.
76. Steriade M., McCormick D. A. and Sejnowski T. J. (1993) Thalamocortical oscillations in the sleeping and aroused brain. *Science* **262,** 679–685.
77. Steriade M., Parent A. and Hada J. (1984) Thalamic projections of nucleus reticularis thalami of cat: a study using retrograde transport of horseradish peroxidase and fluorescent tracers. *J. comp. Neurol.* **229,** 531–547.
78. Tsubokawa H. and Ross W. N. (1997) Muscarinic modulation of spike backpropagation in the apical dendrites of hippocampal CA1 pyramidal neurons. *J. Neurosci.* **17,** 5782–5791.
79. Uhlrich D. and Cucchiaro J. (1992) GABAergic circuits in the lateral geniculate nucleus of the cat. *Prog. Brain Res.* **90,** 171–192.
80. Uhlrich D. J., Tamamaki N. and Sherman S. M. (1990) Brainstem control of response modes in neurons of the cat's lateral geniculate nucleus. *Proc. natn. Acad. Sci. U.S.A.* **87,** 2560–2563.
81. von Krosigk M., Bal T. and McCormick D. (1993) Cellular mechanisms of a synchronized oscillation in the thalamus. *Science* **261,** 361–364.
82. Warren R. A., Agmon A. and Jones E. G. (1994) Oscillatory synaptic interactions between ventroposterior and reticular neurons in mouse thalamus *in vitro*. *J. Neurophysiol.* **72,** 1993–2003.
83. Williams D. (1953) A study of thalamic and cortical rhythms in petit mal. *Brain* **76,** 50–69.
84. Williams S. R., Turner J. P., Anderson C. M. and Crunelli V. (1996) Electrophysiological and morphological properties of interneurones in the rat dorsal lateral geniculate nucleus *in vitro*. *J. Physiol., Lond.* **490,** 129–147.
85. Williams S. R., Turner J. P. and Crunelli V. (1995) Gamma-hydroxybutyrate promotes oscillatory activity of rat and cat thalamocortical neurons by a tonic $GABA_B$ receptor-mediated hyperpolarization. *Neuroscience* **66,** 133–141.
86. Wong M. T. T. (1970) Somato-dendritic and dendro-dendritic synapses in the squirrel monkey lateral geniculate nucleus. *Brain Res.* **20,** 135–139.
87. Yellen G. (1982) Single Ca^{2+} activated nonselective cation channels in neuroblastoma. *Nature* **296,** 357–359.
88. Yuste R. and Denk W. (1995) Dendritic spine as basic functional units of neuronal integration. *Nature* **375,** 682–684.
89. Zhu J. J., Lytton W. W. and Uhlrich D. (1999) Properties of a hyperpolarization-activated cation current in interneurons in the rat lateral geniculate nucleus. *Neuroscience* (in press).
90. Zhu J. J. and Uhlrich D. (1997) Nicotinic receptor-mediated responses in relay cells and interneurons in the rat lateral geniculate nucleus. *Neuroscience* **80,** 191–202.
91. Zhu J. J., Uhlrich D. and Lytton W. W. (1995) Oscillations in thalamic interneurons. *Soc. Neurosci. Abstr.* **21,** 12.5.

(*Accepted* 28 *October* 1998)